

## Effects of ship wakes on ocean brightness and radiative forcing over ocean

C. K. Gatebe,<sup>1,2</sup> E. Wilcox,<sup>3</sup> R. Poudyal,<sup>2,4</sup> and J. Wang<sup>5</sup>

Received 6 July 2011; revised 8 August 2011; accepted 8 August 2011; published 8 September 2011.

[1] Changes in surface albedo represent one of the main forcing agents that can counteract, to some extent, the positive forcing from increasing greenhouse gas concentrations. Here, we report on enhanced ocean reflectance from ship wakes over the Pacific Ocean near the California coast, where we determined, based on airborne radiation measurements that ship wakes can increase reflected sunlight by more than 100%. We assessed the importance of this increase to climate forcing, where we estimated the global radiative forcing of ship wakes to be  $-(0.14 \pm 50\%) \text{ mWm}^{-2}$  assuming a global distribution of 32331 ships of size  $\geq 100000$  gross tonnage. The forcing is smaller than the forcing of aircraft contrails ( $-0.007$  to  $+0.02 \text{ Wm}^{-2}$ ), but considering that the global shipping fleet has rapidly grown in the last five decades and this trend is likely to continue because of the need of more intercontinental transportation as a result of economic globalization, we argue that the radiative forcing of wakes is expected to be increasingly important especially in harbors and coastal regions. **Citation:** Gatebe, C. K., E. Wilcox, R. Poudyal, and J. Wang (2011), Effects of ship wakes on ocean brightness and radiative forcing over ocean, *Geophys. Res. Lett.*, 38, L17702, doi:10.1029/2011GL048819.

### 1. Introduction

[2] The oceanic surface albedo plays a key role in determining the energy exchange between atmosphere and ocean, and is therefore important for the coupling of atmosphere and ocean models [Li *et al.*, 2006]. The albedo regulates Earth's climate, and an increase in surface albedo can counteract, to some extent, the warming due to the positive forcing of increasing greenhouse gases [Menon *et al.*, 2010]. The albedo change over land caused by land-use and land-cover modifications is well documented [Forster *et al.*, 2007]. However, modification of the ocean albedo by human activities is unknown, even though the oceans cover 70% of Earth's surface and absorbs approximately 93% of incident solar radiation. It is therefore conceivable that increasing surface albedo by adding micro-bubbles can reduce heat oceanic uptake and potentially counterbalance human-induced warming from landscape darkening and emission of black carbon and greenhouse gases as argued recently by Seitz [2011]. This study provides new insights into ship-generated disturbances

on the ocean surface, which have received little attention in climate studies, but is potentially significant for the ocean-atmosphere energy balance and could affect climate.

[3] A moving ship generates a wake that is characterized by surface waves, white-water, propeller-generated vortices, and submerged bubbles [Reed and Milgram, 2002]. Ship wakes can often be seen in images acquired by microwave synthetic aperture radar (SAR) aboard aircraft and satellites [Garzelli, 1995; Munk *et al.*, 1987]. The region around and behind the ship up to a distance of several ship lengths (local wave disturbance region) shows a complex combination of breaking bow and stern waves, depending on the speed, the shape, and the propulsion system of the ship [Lyden *et al.*, 1988]. Studies have shown that the optical variations observed within ship wakes are largely due to the generation of copious amounts of air bubbles in the upper ocean, a fraction of which accumulate as foam at the surface, where they release scavenged surfactants [Zhang *et al.*, 2004, 1998; Stramski, 1994]. The optical effects of surface waves, submerged bubbles, and vortices trailing the ship can be observed 5–15 km behind the ship [Munk *et al.*, 1987].

### 2. Observational Assessment of Ship Wake Impacts on Surface Albedo

[4] During the Arctic Research of the Composition of the Troposphere from Aircraft and Satellites (ARCTAS; 24 June 2008) experiment [Jacob *et al.*, 2010], while flying in the NASA P-3B aircraft (Figure 1a) over the Pacific Ocean off the coast of southern California, we observed, serendipitously, enhanced surface reflectance exceeding 100% above normal in most cases in wakes trailing large commercial vessels. The flight was designed primarily for characterizing the emissions from cargo ships plying the area, which are known to contribute to air quality problems in California [Corbett and Fischbeck, 2000; Corbett *et al.*, 2007], and the ocean bidirectional reflectance distribution function (BRDF). The aircraft was equipped with instruments to measure gases, aerosols and radiation. As part of the instrument suite, the NASA's Cloud Absorption Radiometer (CAR; Figure 1b) [Gatebe *et al.*, 2003; King *et al.*, 1986], which detected the enhanced reflectance, was mounted in the nose cone measuring both transmitted and reflected radiances while scanning perpendicular to the flight direction at a rate of 100 scans a minute. CAR scans through  $190^\circ$  from straight above, through the horizon to straight down. Data were recorded for 14 narrow spectral bands located in the ultraviolet, visible and near-infrared regions in the electromagnetic spectrum (0.340–2.301  $\mu\text{m}$ ). (Data and information supporting our results are available online at the CAR website ([http://car.gsfc.nasa.gov/data/index.php?id=122&mis\\_id=8&n=ARCTAS](http://car.gsfc.nasa.gov/data/index.php?id=122&mis_id=8&n=ARCTAS)). Given that the instrument has an instantaneous

<sup>1</sup>Goddard Earth Sciences Technology and Research, Universities Space Research Association, Columbia, Maryland, USA.

<sup>2</sup>NASA Goddard Space Flight Center, Greenbelt, Maryland, USA.

<sup>3</sup>Desert Research Institute, Reno, Nevada, USA.

<sup>4</sup>Science Systems and Applications, Inc., Lanham, Maryland, USA.

<sup>5</sup>Department of Earth and Atmospheric Sciences, University of Nebraska-Lincoln, Lincoln, Nebraska, USA.

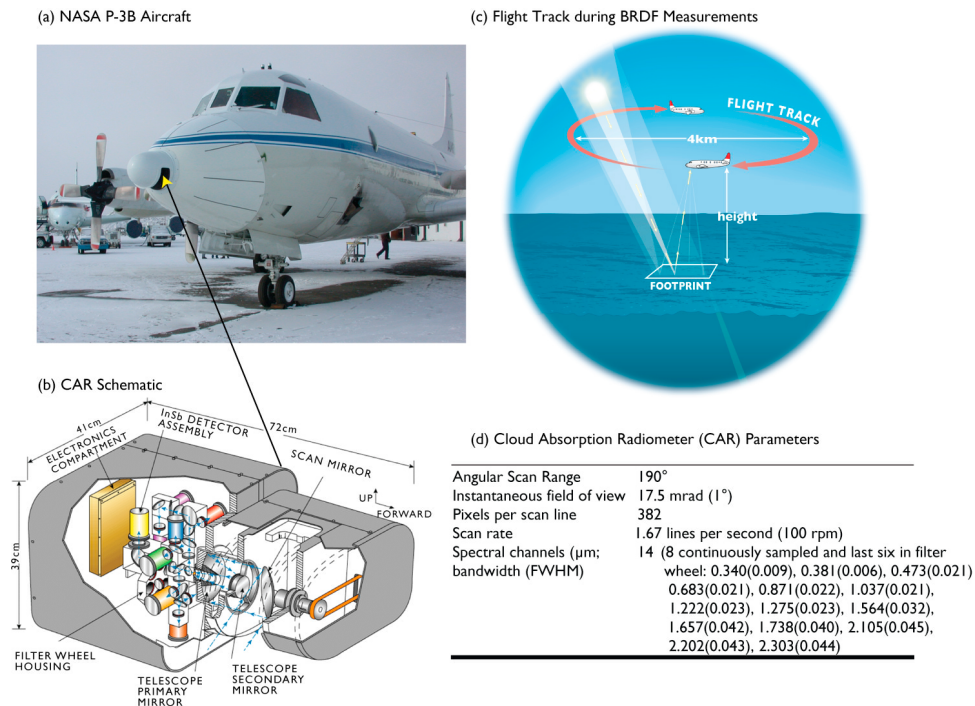


**Figure 1.** (a) The NASA P-3B at Fairbanks, Alaska, USA in April 2008 during ARCTAS Field Experiment. (b) Schematic of NASA's Cloud Absorption Radiometer (CAR), which is mounted in the nose cone of the NASA P-3B aircraft. (c) Illustration of a clockwise circular flight track that was used for measuring surface bidirectional reflectance distribution function (BRDF) over the Pacific. (d) The CAR has 14 narrow spectral bands between 0.34 and 2.30  $\mu\text{m}$ , and flew two missions over the Pacific during ARCTAS.

field-of-view of 1°, a wide scan range of 190°, and assuming an altitude of 300 m above the surface, the diameter of the footprint straight below the aircraft is  $\sim 5$  m, increasing to  $\sim 174$  m at a viewing zenith angle of 80° from nadir. Therefore, a complete circular orbit by the aircraft allows the CAR to image the surface and sky in all viewing zenith and azimuthal angles, and covering an area defined by a diameter of 4–5 km on the surface (Figure 1c). We believe that using the CAR in this manner is the most mobile and efficient way of measuring full surface BRDF assuming a homogeneous surface [Gatebe *et al.*, 2005]. Several orbits over ocean were completed both before and after the arrival of a ship to the sampling area, presenting us with unprecedented opportunity to detect change in surface albedo due to ship wakes.

[5] The signature of the ship and its wake can be seen clearly when comparing the BRDF of the case without and with ship wake. We use measurements of BRDF to determine the enhanced reflectance attributable to the presence of ship wake. Figure 2 shows ocean reflectance at 0.870  $\mu\text{m}$  in all viewing azimuth directions (depicted as angle around the polar plot with the solar principal plane at 0°) and viewing zenith angle (depicted as distance from the center of the polar plot) from nadir up to 10° below the horizon. At 0.870  $\mu\text{m}$ , which is widely used in remote sensing over the ocean under clear-sky, effects of atmospheric absorption and scattering can be assumed to be minimal. The unique feature of these BRDF measurements is that reflected solar radiation was observed at a fine angular resolution (1°). As expected, the radiation field over the ocean is characterized by the presence of sunglint with maximum reflectance coinciding with the solar direction (in this case  $\sim 35^\circ$  elevation angle) viewed

towards the sun and minimum reflectance occurring at the same elevation angle viewed away from the sun caused by the aircraft shadow. However, the contrast between Figure 2a (case without ship wake) and Figure 2b (case with the ship wake) reveals: (a) ship and ship wakes clearly enhance surface reflectance, (b) the glint is confined over a narrower angular range from the solar principal plane in the ship wake case, and extends farther out towards the horizon, and (c) the

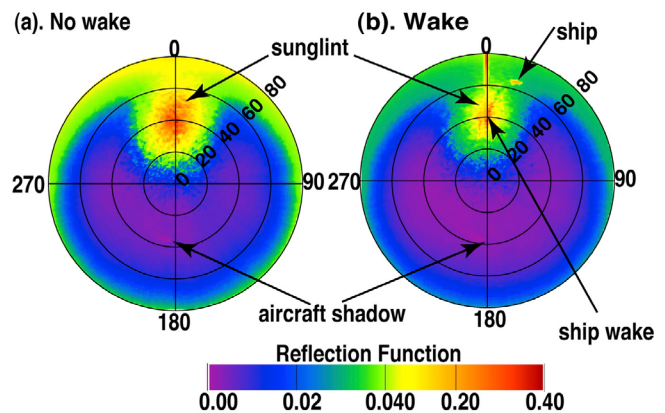


**Figure 2.** Ocean bidirectional reflectance distribution function at 0.870  $\mu\text{m}$  (a) without and (b) with ship wake. The ship wake measurements were made over a 294 m long cargo ship, which was moving through an area where the NASA P-3B aircraft was orbiting in a circular flight track at a constant altitude ( $\sim 304$  m above ocean surface).

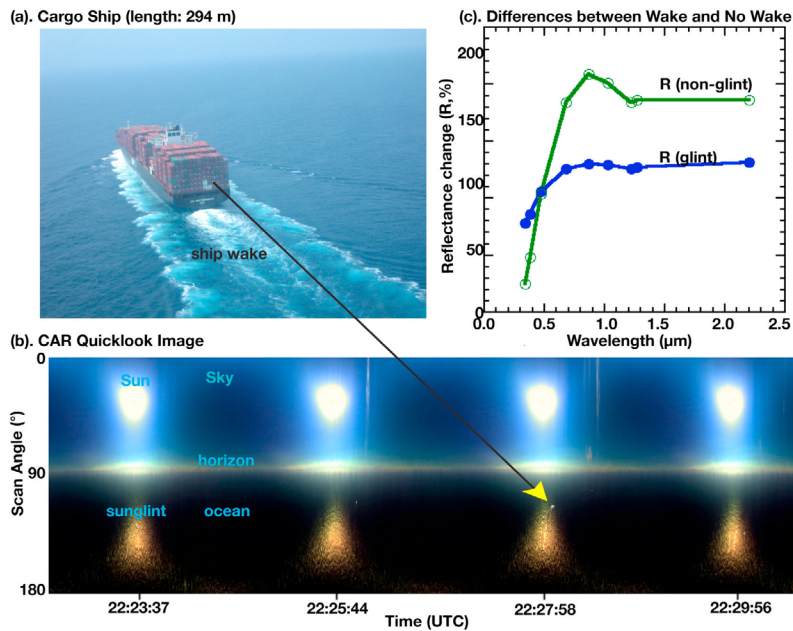


**Figure 3.** (a) Cargo ship moving through the scene during airborne measurements. (b) The cargo ship can be seen in a quick-look image from NASA’s Cloud Absorption Radiometer. (c) Relative change in reflectance in the solar principal plane ( $R_{\text{glint}}$ ) and off-principal plane ( $R_{\text{non-glint}}$ ) due to the presence of ship wake.

glint in the ship wake case has higher reflectance magnitude than the non-ship wake case, which is not so obvious in the figure because of the color scheme used. The narrowing of the angular extent of the glint and the reduction in reflectance in some viewing angles is more than compensated by enhanced surface reflectance at other viewing angles.

[6] The ship passage (Figure 3a) captured by the CAR instrument during a  $\sim 2$  minute interval as seen in the quick-look RGB image shown in Figure 3b ( $R = 1.04 \mu\text{m}$ ,  $G = 0.87 \mu\text{m}$ , and  $B = 0.47 \mu\text{m}$ ) triggered our initial interests in reflectance enhancement by ship wake. The sun can be seen in the sky, well above the horizon, and the sunglint pattern appears very bright against a dark ocean surface. The ship and its wake appear in the quick-look image more clearly at 22:27:58 UTC. The ship appears as a bright dot off the solar principal plane and the ship wake is superimposed on the glint following the ship. Figure 3c (blue curve) shows the mean percentage differences in spectral surface reflectance viewed in the direction of the sunglint between the case with ship wake (22:27:58 UTC–22:29:56 UTC) and the case without the wake (22:23:37 UTC–22:25:44 UTC), normalized to the case without the wake. The green line in Figure 3c, is similar to the blue line, but for a different ship wake viewed in non-glint directions  $>90^\circ$  away from the solar principal plane. We identified other ship wakes associated with trailing ships of varying size and observed by CAR at different distances and altitudes above the ocean surface. Table 1 shows results of differences in spectral reflectance ( $\Delta R$ ) between the case with ship wake and the case without, expressed in the general form:

$$\Delta R = \frac{\pi \Delta I_\lambda(\theta, \theta_0, \phi)}{\mu_0 F_\lambda} \quad (1)$$

where  $\theta$  and  $\theta_0$  are the viewing and illumination zenith angles, respectively,  $\phi$  is the azimuthal angle between the

viewing direction and the illumination direction so that forward and backward scattered photons represent azimuth angles of  $0^\circ$  and  $180^\circ$ , respectively,  $\mu = \cos \theta$ ,  $\mu_0 = \cos \theta_0$ ,  $\Delta I_\lambda(\langle \mu \rangle (\langle I_{\lambda,w} \rangle - \langle I_\lambda \rangle))$  is the absolute differences in measured radiance between the case with ship wake ( $I_{\lambda,w}$ ) and the case without the wake ( $I_\lambda$ ), averaged over different pixels, and multiplied with  $\mu$ .  $F_\lambda$ , the collimated irradiance, is computed by weighting the solar flux at the top of the atmosphere with the spectral response function of each band, taking into account the effects of the elliptical orbit of the Earth around the Sun. (Note that results for ship wake 1 and 4 are shown in Figure 3c (green and blue curves, respectively).) Enhanced reflectances were measured across the spectrum from UV to near-IR for all observed wakes, with considerable variability observed between different wakes, especially between glint and non-glint cases (cf. Table 1 - standard error estimate). Note that the relative change in reflectance is greater at longer wavelengths. This may be explained by the decreasing reflectance with increasing wavelength of the ocean being enhanced by additional scattering by bubbles, which is roughly uniform across the visible/NIR spectrum. This spectral signature of the ship wakes is qualitatively similar to that observed by Zhang *et al.* [2004].

[7] It is straightforward to estimate the actual wake area associated with the ship. We used unsupervised classification algorithm - ISODATA in ENVI [cf. Jensen, 1996] to select pixels disturbed by the wake around the general location of a ship identified in the CAR quick-look image. The dimensions of individual pixels were determined using geometrical methods [cf. Román *et al.*, 2011, equations 1–10]. Assuming the ocean to be Lambertian, we derived broadband albedo from the spectral values in Table 1 using a modified conversion formula by Liang *et al.* [2005] for MODIS (Moderate-Resolution Imaging Spectroradiometer) bands, which predicts average shortwave broadband ( $0.2\text{--}2.5 \mu\text{m}$ )

**Table 1.** Increase in Ocean-Atmosphere Nadir Spectral Reflectance due to Ship Wake<sup>a</sup>

	0.340	0.381	0.472	0.682	0.870	1.036	1.219	1.273	2.102	Alt (m)/SZA(°)/N
Ship-1	0.0056 ± 0.0017	0.0107 ± 0.0009	0.0157 ± 0.0026	0.0144 ± 0.0026	0.0133 ± 0.0026	0.0116 ± 0.0023	0.0097 ± 0.0017	0.0096 ± 0.0015	0.0071 ± 0.0012	7062/17/118
Ship-2	0.0050 ± 0.0007	0.0095 ± 0.0015	0.0135 ± 0.0025	0.0096 ± 0.0024	0.0078 ± 0.0022	0.0063 ± 0.0020	0.0046 ± 0.0015	0.0046 ± 0.0015	0.0014 ± 0.0006	7096/16/104
Ship-3	0.0223 ± 0.0011	0.0310 ± 0.0024	0.0354 ± 0.0040	0.0315 ± 0.0047	0.0276 ± 0.0046	0.0240 ± 0.0041	0.0182 ± 0.0033	0.0175 ± 0.0031	0.0074 ± 0.0016	2186/20/181
Ship-4 (glint)	0.0095 ± 0.0007	0.0174 ± 0.0013	0.0321 ± 0.0019	0.0435 ± 0.0025	0.0518 ± 0.0032	0.0613 ± 0.0025	0.0591 ± 0.0036	0.0451 ± 0.0021	0.0503 ± 0.0034	299/35/605

<sup>a</sup>R<sub>w</sub> = ship wake spectral nadir reflectance, R = ocean spectral nadir reflectance; SZA = solar zenith angle, and N is the number of pixels contaminated by ship wake. The estimated shortwave (0.25–2.5 μm) broadband albedo enhancement: ship-1 = 0.0116; ship-2 = 0.0077, ship-3 = 0.0190, ship-4 (glint case) = 0.0417. The ship wake area (km<sup>2</sup>): ship-1 = 0.4820, ship-2 = 0.4880, ship-3 = 0.9284, ship-4 = 0.2706.

albedo of any surface type, under general atmospheric conditions, and assuming that downward fluxes beyond this range are very small and their contribution to the total albedo are negligible. This gives an equivalent broadband albedo increase as shown in Table 1. Clearly, the albedo enhancement is stronger in the glint case than the non-glint cases.

### 3. Estimate and Significance of Direct Radiative Forcing of Ship Wakes

[8] We now explore the impact on climate associated with the strong increase of albedo by ship wakes as a primer for any future work. We adopt an approach similar to *Charlson et al.* [1992] for sulfate aerosols, *Penner et al.* [1992] for biomass burning aerosols, *Frouin et al.* [2001] for oceanic whitecaps, and *Seitz* [2011] for oceanic micro-bubbles to assess the climatic role of ship wakes on a global scale. The conceptual simplicity of this approach makes it more attractive and convenient to use for a rough order estimate of the direct radiative forcing of ship wakes.

[9] Ship wake brightening is largely attributed to copious amounts of air bubbles in the upper ocean, which increase backscattering and enhance reflectance over the entire ultraviolet, visible and near infrared wavelengths (cf. Figure 3). Therefore, air bubbles in the upper ocean can be treated as spherical voids in the water column similar to aerosol or water droplets suspended in air. Consequently, the formalism used to express the degree of planetary brightening  $\Delta F$  from aerosols in the atmosphere can be applied as well to hydrosol clouds in ocean. Therefore, the change in outgoing radiative flux due to ship wake at any location over the oceans is given by:

$$\Delta F = -F_0 \mu_0 (1 - A_c) t^u t^d \Delta R_s \quad (2)$$

Where  $F_0$  is the extraterrestrial broad-band solar irradiance,  $\mu_0$  is the cosine of the solar zenith angle,  $A_c$  is the fraction of the surface covered by clouds,  $t^u$  and  $t^d$  are clear sky transmissivities for up- and downwelling fluxes, respectively, and  $\Delta R_s$  is the change in the albedo of the upper water column that ship wake bubbles produce. We assume that the forcing occurs only in cloud-free regions and the atmosphere-surface interactions are neglected.

[10] The  $\Delta R_s$  can be obtained from the following expression:

$$\Delta R_s = N f_w (R_w - R) \quad (3)$$

Where N is the number of ships,  $f_w$  denotes the fraction of surface covered by ship wakes,  $R_w$  is the total broadband surface reflectance from ship wakes (sum of contributions due to diffuse reflection by air bubbles, whitecaps, and rough ocean surfaces), and  $R$  is total broadband reflectance from ship wake-free surfaces. The total broadband albedo perturbation are given in Table 1 for different ships. Given the variability in the observed albedo enhancements between glint and non-glint wake cases reported in Table 1 (footnote), we weighted the albedo enhancement by the wake area for purposes of RF computation.

[11] The number of ships, N, is based on several sources, for example, *Eyring et al.* [2005] who reported 89063 ships exceeding 100 gross tonnage (excluding submarines) in 2001 operating between 4000 and 6600 hours per year depending

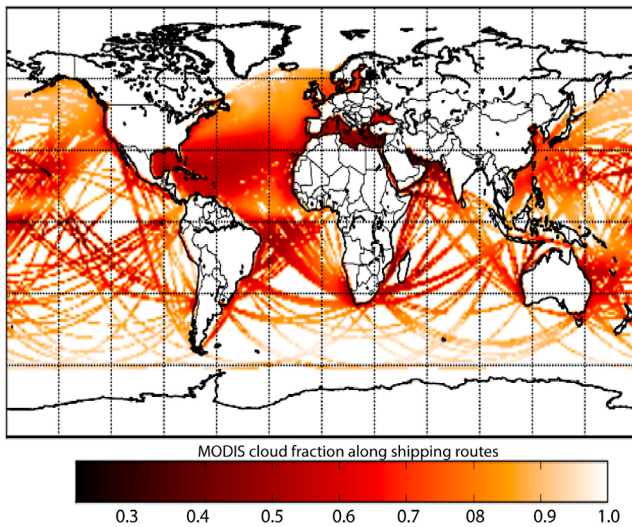


**Figure 4.** Average cloud fraction along global shipping routes as computed from Moderate Resolution Imaging Spectrometer (MODIS) data acquired from the Terra satellite (2001–2010). The average cloud fraction over global shipping routes is 0.71.

on size. Allowing that 40% of that operating time may be stationary in port [Endresen *et al.*, 2003] yields between 24400 and 40261 ships operating in open water at any time. If we use the average number of ships (32331), the uncertainty in our estimate of the number of ships is  $\pm 24\%$ . Note that the size of the fleet has quadrupled in approximately 50 years [Buhaug *et al.*, 2009].

[12] The average cloud fraction along global shipping routes is computed from 10 years of Moderate Resolution Imaging Spectrometer (MODIS) data acquired from the Terra satellite for years 2001 through 2010. The one degree gridded monthly data are taken from the MOD08\_M3 (version 5.1) product supplied by NASA. The 10-year average of these data are shown in Figure 4 masked by one-degree grid cells within shipping routes determined from Kaluza *et al.* [2010]. The average cloud fraction over global shipping routes is 0.71. There is little difference between this quantity and that of the 8-year average of MODIS data from the Aqua satellite similarly masked by shipping routes. The density of ship traffic is not uniform between shipping lanes. Lacking adequate data for ship density, it was not possible to compute an average of cloud fraction weighted by ship traffic density. However, the standard deviation of cloud fraction across all samples within shipping lanes is 0.14, which we adopt here as a conservative estimate of the uncertainty in the masking of ship wake radiative forcing by clouds. Note that the global cloud field is extremely stable over the >10 years MODIS data record with seasonal and diurnal variation of global cloud cover change of approximately 2% [Maddux *et al.*, 2010].

[13] The clear-sky atmospheric transmittance (0.76) and its relative uncertainty (20%) are taken from Charlson *et al.* [1992, Table 1]. Therefore, the two-way clear-sky atmospheric transmittance  $0.58 \pm 40\%$ . The solar constant variations are considered too small ( $<0.01\%$  [e.g., Beer *et al.*, 2000]) to affect the ship wake forcing estimate.

[14] Using equations (2) and (3) the globally averaged perturbation in reflected solar flux due to the presence of ship wakes can be estimated:

$$\langle \Delta F \rangle = -0.25F_0(1 - \langle A_c \rangle)T\langle N \rangle\langle f \rangle\langle \Delta R_s \rangle \quad (4)$$

where  $\langle \rangle$  denotes globally averaged values over the ocean (simple average area),  $0.25F_0$  is the global mean top-of-the-atmosphere radiative flux ( $0.25 \times 1367 \text{ Wm}^{-2}$ ),  $\langle A_c \rangle$  is the globally averaged MODIS fractional cloud coverage (0.71),  $T$  is the clear-sky two-way atmospheric transmittance (0.58 from Charlson *et al.* [1992]),  $\langle N \rangle$  is the average number of ships (32331),  $\langle f \rangle$  is the sum of the average wake area divided by total area of the Earth ( $2.17/5.1 \times 10^8$ ),  $\Delta R_s$  is the area weighted albedo enhancement (0.018). Using these estimates the probable  $\langle \Delta F \rangle$  is  $-(0.00014 \pm 0.00007) \text{ Wm}^{-2}$ . This calculation assumes that ship wakes are homogeneously distributed over the globe. However, since the majority of ships are in the northern hemisphere mid-latitude oceans, the estimate averaged over the globe would be  $-0.00014 \text{ Wm}^{-2} \times 0.5$  (hemispheric factor)  $\times \cos\pi/4$  (mid-latitude factor)  $= -0.000049 \text{ Wm}^{-2}$ . Consequently, the forcing averaged only over the northern hemisphere ocean would be  $\sim -0.00016 \text{ Wm}^{-2}$  (noting that ocean surface area in northern hemisphere is  $\sim 30\%$  of the total Earth's surface area). Regionally, in harbours and coastal regions, we would expect the forcing to be much larger.

[15] Therefore, globally, the above estimate of ship wake forcing ( $-0.00014 \text{ Wm}^{-2}$ ) is much smaller than aircraft contrails forcing, which lie in the range  $-0.007$  to  $+0.02 \text{ Wm}^{-2}$  [Forster *et al.*, 2007]. These estimates are designed to be illustrative of the potential magnitude of forcing by ship wakes. Despite the uncertainty in the above estimate of ship wake forcing due to considerable uncertainty in the input parameters as indicated, the calculation serves to establish the significance of the direct forcing of the ship wakes.

#### 4. Conclusions

[16] The strong enhancement of ocean reflectance in the ship wake is unambiguous, and  $>100\%$  in most cases in the spectral range from the ultraviolet to the near-infrared ( $0.340 \mu\text{m} \leq \lambda \leq 2.205 \mu\text{m}$ ), and clearly seen in the ocean BRDF measurements. These results are derived from angular and spectral measurements of the intensity of reflected solar radiation from an airborne instrument over several regions of the ocean disturbed by the ship wakes. The implication for the global radiation budget at the top of the atmosphere has been demonstrated in this study. Wherever possible we have taken the nominal values for all parameters in our radiative forcing estimate for ship wakes. We acknowledge that some parameters may have large and as yet difficult-to-quantify uncertainties and therefore, ship wake forcing may turn out to be nothing, but there is a real possibility that it could turn out to be something. Further sampling of ship wakes is warranted to better constrain the estimated change in albedo from wakes and to improve our understanding of the persistence of the albedo perturbation after passage of the ship. Hence, the forcing estimate here ( $-0.14 \pm 50\%$ )  $\text{mWm}^{-2}$  should be considered as a first order estimate (or back-of-the-envelope estimate), whereby uncertainties could be as large as those in the forcing estimate for

aerosol or even contrails. But, considering that the global shipping fleet has rapidly grown in the last five decades and this trend is likely to continue because of the need of more inter-continental transportation as a result of economic globalization, we argue that the radiative forcing of wakes is expected to be increasingly important and could have bearing on the suggested geo-engineering schemes (such as using cloud modifying ships) for reducing warming [e.g., MacCracken, 2009; Seitz, 2011]. Studies [e.g., Buhaug et al., 2009] show that, by 2050, in the absence of policies, ship emissions may grow by 150% to 250% (compared to the emissions in 2007) as a result of the growth in shipping.

[17] **Acknowledgments.** This research was supported by the Science Mission Directorate of the National Aeronautics and Space Administration as part of the Radiation Sciences Program under Hal B. Maring and Airborne Science Program, Bruce Tagg. This work was performed under NASA grant NNX08AF89G. We thank the editors and two anonymous reviewers for their valuable comments.

[18] The Editor thanks two anonymous reviewers for their assistance in evaluating this paper.

## References

- Beer, J., W. Mende, and R. Stellmacher (2000), The role of the Sun in climate forcing, *Quat. Sci. Rev.*, *19*, 403–415, doi:10.1016/S0277-3791(99)00072-4.
- Buhaug, Ø., et al. (2009), Second IMO GHG study, Prevention of air pollution from ships, Int. Marit. Organ., London.
- Charlson, R. J., S. E. Schwartz, J. M. Hales, R. D. Cess, J. A. Coakley, J. E. Hansen, and D. J. Hofmann (1992), Climate forcing by anthropogenic aerosols, *Science*, *255*, 423–430, doi:10.1126/science.255.5043.423.
- Corbett, J. J., and P. S. Fischbeck (2000), Emissions from waterborne commerce in United States continental and inland waters, *Environ. Sci. Technol.*, *34*, 3254–3260, doi:10.1021/es9911768.
- Corbett, J. J., J. Firestone, and C. Wang (2007), Estimation, validation, and forecasts of regional commercial marine vessel inventories, final report, Calif. Air Resour. Board, Sacramento. [Available at <http://www.arb.ca.gov/research/seca/jcfinal.pdf>.]
- Endresen, Ø., E. Sørsgård, J. K. Sundet, S. B. Dalsøren, I. S. A. Isaksen, T. F. Berglen, and G. Gravir (2003), Emission from international sea transportation and environmental impact, *J. Geophys. Res.*, *108*(D17), 4560, doi:10.1029/2002JD002898.
- Eyring, V., H. W. Köhler, J. van Aardenne, and A. Lauer (2005), Emissions from international shipping: 1. The last 50 years, *J. Geophys. Res.*, *110*, D17305, doi:10.1029/2004JD005619.
- Forster, P., et al. (2007), Changes in atmospheric constituents and in radiative forcing, in *Climate Change 2007: The Physical Science Basis. Contribution of Working Group I to the Fourth Assessment Report of the Intergovernmental Panel on Climate Change*, edited by S. Solomon et al., pp. 129–234, Cambridge Univ. Press, Cambridge, U. K.
- Frouin, R., S. F. Jacobellis, and P.-Y. Deschamps (2001), Influence of oceanic whitecaps on the global radiation budget, *Geophys. Res. Lett.*, *28*, 1523–1526, doi:10.1029/2000GL012657.
- Garzelli, A. (1995), Detection of ship wakes in SAR images using morphological operators, *Comput. Geosci.*, *21*, 1201–1203, doi:10.1016/0098-3004(95)00051-8.
- Gatebe, C. K., M. D. King, S. Platnick, G. T. Arnold, E. F. Vermote, and B. Schmid (2003), Airborne spectral measurements of surface-atmosphere anisotropy for several surfaces and ecosystems over southern Africa, *J. Geophys. Res.*, *108*(D13), 8489, doi:10.1029/2002JD002397.
- Gatebe, C. K., M. D. King, A. I. Lyapustin, G. T. Arnold, and J. Redemann (2005), Airborne spectral measurements of ocean directional reflectance, *J. Atmos. Sci.*, *62*, 1072–1092, doi:10.1175/JAS3386.1.
- Jacob, D. J., et al. (2010), The Arctic Research of the Composition of the Troposphere from Aircraft and Satellites (ARCTAS) mission: Design, execution, and first results, *Atmos. Chem. Phys.*, *10*, 5191–5212, doi:10.5194/acp-10-5191-2010.
- Jensen, J. R. (1996), *Introductory Digital Image Processing—A Remote Sensing Perspective*, pp. 197–256, Prentice Hall, Upper Saddle River, N. J.
- Kaluza, P., A. Kölzsch, M. T. Gastner, and B. Blasius (2010), The complex network of global cargo ship movements, *J. R. Soc. Interface*, *7*, 1093–1103, doi:10.1098/rsif.2009.0495.
- King, M. D., M. G. Strange, P. Leone, and L. R. Blaine (1986), Multiwavelength scanning radiometer for airborne measurements of scattered radiation within clouds, *J. Atmos. Oceanic Technol.*, *3*, 513–522, doi:10.1175/1520-0426(1986)003<0513:MSRFAM>2.0.CO;2.
- Li, J., J. Scinocca, M. Lazare, N. McFarlane, K. Von Salzen, and L. Solheim (2006), Ocean surface albedo and its impact on radiation balance in climate models, *J. Clim.*, *19*, 6314–6333, doi:10.1175/JCLI3973.1.
- Liang, S., Y. Yu, and T. P. Defelice (2005), VIIRS narrow to broadband land surface albedo convergence formula and validation, *Int. J. Remote Sens.*, *26*, 1019–1025, doi:10.1080/01431160512331340156.
- Lyden, J. D., R. R. Hammond, D. R. Lyzenga, and R. A. Shuchman (1988), Synthetic aperture radar imaging of surface ship wakes, *J. Geophys. Res.*, *93*, 12,293–12,303, doi:10.1029/JC093iC10p12293.
- MacCracken, M. C. (2009), On the possible use of geoengineering to moderate specific climate change impacts, *Environ. Res. Lett.*, *4*, 045107, doi:10.1088/1748-9326/4/4/045107.
- Maddux, B. C., S. A. Ackerman, S. Platnick, and W. Menzel (2010), The vertical and horizontal distribution of clouds and uncertainty from MODIS, Abstract A43B-0227 presented at Fall Meeting, AGU, Washington, D. C., 13–17 Dec.
- Menon, S., H. Akbari, S. Mahanama, I. Sednev, and R. Levinson (2010), Radiative forcing and temperature response to changes in urban albedos and associated CO<sub>2</sub> offsets, *Environ. Res. Lett.*, *5*, 014005, doi:10.1088/1748-9326/5/1/014005.
- Munk, W. H., P. Scully-Power, and F. Zachariassen (1987), Ships from space, *Proc. R. Soc. London, Ser. A*, *412*, 231–254, doi:10.1098/rspa.1987.0087.
- Penner, J. E., R. E. Dickinson, and C. A. O'Neill (1992), Effects of aerosol from biomass burning on the global radiation budget, *Science*, *256*, 1432–1434, doi:10.1126/science.256.5062.1432.
- Reed, A. M., and J. H. Milgram (2002), Ship wakes and their radar images, *Annu. Rev. Fluid Mech.*, *34*, 469–502, doi:10.1146/annurev.fluid.34.090101.190252.
- Román, M. O., C. K. Gatebe, C. Schaaf, R. Poudyal, Z. Wang, and M. D. King (2011), variability of BRDF at different spatial scales (30 m–500 m) over a mixed agricultural landscape from airborne and satellite spectral measurements, *Remote Sens. Environ.*, *115*(9), 2184–2203, doi:10.1016/j.rse.2011.04.012.
- Seitz, R. (2011), Bright water: hydrosols, water conservation and climate change, *Clim. Change*, doi:10.1007/s10584-010-9965-8, in press.
- Stramski, D. (1994), Gas microbubbles, an assessment of their significance to light scattering in quiescent seas, *Proc. SPIE*, *2258*, 704–710, doi:10.1117/12.190117.
- Zhang, X., M. R. Lewis, and B. D. Johnson (1998), Influence of bubbles on scattering of light in the ocean, *Appl. Opt.*, *37*, 6525–6536, doi:10.1364/AO.37.006525.
- Zhang, X., M. Lewis, W. P. Bissett, B. Johnson, and D. Kohler (2004), Optical influence of ship wakes, *Appl. Opt.*, *43*, 3122–3132, doi:10.1364/AO.43.003122.

C. K. Gatebe and R. Poudyal, NASA Goddard Space Flight Center, Mail Code 613.2, Greenbelt, MD 20771, USA. (charles.k.gatebe@nasa.gov)

J. Wang, Department of Earth and Atmospheric Sciences, University of Nebraska-Lincoln, 303 Bessey Hall, Lincoln, NE 68588-0340, USA.

E. Wilcox, Desert Research Institute, 2215 Raggio Pkwy., Reno, NV 89512, USA.